Architectural modifications for flexible supercapacitor performance optimization

Jari Keskinen[1], Suvi Lehtimäki[1], Arman Dastpak[1], Sampo Tuukkanen[2], Timo Flyktman[3], Thomas M. Kraft[1], Anna Railanmaa[1], Donald Lupo[1]

[1]Tampere University of Technology, Electronics and Communications Engineering, Korkeakoulunkatu 3, FI-33720 Tampere, Finland

[2]Tampere University of Technology, Automation Science and Engineering, Korkeakoulunkatu 3, FI-33720 Tampere, Finland

[3]VTT Technical Research Centre of Finland Ltd, Sinitaival 6, FI-33720 Tampere, Finland

Abstract

We have developed various material and architectural alternatives for flexible supercapacitors and compared their effect on practical performance. The substrate alternatives include paperboard as well as various polyethylene terephthalate (PET) films and laminates with aqueous NaCl electrolyte used in all components. In all the supercapacitors, activated carbon is used in the active layer with graphite ink being used in the current collectors with various aluminium or copper structures applied to enhance the current collectors' conductivity. The capacitance of the supercapacitors was found to lie between 0.085 F and 0.58 F and their equivalent series resistance (ESR) was from below 1 Ω to 14 Ω depending mainly on the current collector structure. Furthermore, leakage current and self-discharge rates were defined and compared for the various architectures. In fact, the barrier properties of the supercapacitor encapsulation have a clear correlation with leakage current, which was clearly shown by the lower

leakage in components with an aluminium barrier layer. A cycle life test showed that after 40000 charge-discharge cycles the capacitance decreases by less than 10 %.

Keywords

Supercapacitor, electric double-layer capacitor, energy storage, substrate, current collector, aqueous electrolyte

1. Introduction

Supercapacitors [1,2] also called electric double layer capacitors (EDLC), are able to meet high peak power requirements of energy storage applications. A supercapacitor consists of two electrodes separated by an ionically conductive electrolyte. The electrolyte is impregnated into the electrodes, between which a porous separator is located. The electrodes are typically made of activated carbon (AC) powder that is bound using fluorine containing polymers such as polytetrafluoroethylene (PTFE) or polyvinylidene fluoride (PVDF). Organic solutions such as propylene carbonate or acetonitrile are typically used, but it is also possible to use water based electrolytes. With organic electrolytes a maximum voltage of about 2.5 V can be applied between the electrodes, whereas with water based electrolytes the maximum voltage is limited to about 1.2 V.

Different measurement, identification and data storage/transfer devices as well as miniaturized sensors are essential components in Internet of Things (IoT) applications. Active RFID tags and sensors require a suitable power source to fully utilize their potential for greater memory capacity and increased reading distance [3]. Since these tags are often intended to be used as integrated parts of recyclable products, all components of the power source/RFID tag/sensor combination should be biodegradable or incinerable when the product is disposed together with normal household waste. It has been shown

that supercapacitors can be manufactured from environmentally friendly materials [4–8]. Further, to facilitate application of these devices in large scale, they should be fabricated using inexpensive materials and manufacturing methods. Traditional battery technology can rarely fulfill these requirements.

As well as being made from environmentally friendly materials and by means of potentially printable fabrication processes, an attractive aspect of these supercapacitors is their mechanical flexibility [9]. Flexible electronics have evolved significantly from flexible circuits, in which printed wiring was utilized on flexible substrates, to flexible components. The advent of third generation electronics have provided a means for printable, thin, and flexible devices, such as solar cells [10], batteries [11], sensors [12] and supercapacitors [6,13,14]. Furthermore, with the incorporation of the graphite electrodes a great deal of flexibility is achieved with future with future endeavors leading to stretchable devices [15]. The ease in which the supercapacitors can be incorporated into various applications, be it wearables or nearables, is enhanced with their inherent flexibility.

The components of an EDLC can be made by printing techniques which makes single stage manufacturing and integration with other printed electronics components feasible. This enables for example high throughput manufacturing energy harvesting circuits [16,17]. The manufacturing of supercapacitor electrodes using printing techniques has been described in patent and scientific literature [5–7,18–27]. Solution based processes that can be modified to screen printing have been reported in the preparation of polyaniline or polypyrrole based supercapacitors [28,29]. Batteries and supercapacitors of carbon nanotubes and room-temperature ionic liquid electrolytes have been constructed using paper as substrate material [30].

Th objective of our work has been to develop supercapacitors for “Internet of Things” (IoT) and wireless sensor network applications. The amount of these systems continues to increase and the number of

connected objects will grow drastically. For this to be possible, a shift from current approaches where batteries are used is needed. In the future, IoT objects will have to be extremely low cost, flexible and thin in order for this ubiquitous electronics to be unobtrusive. They are autonomous devices that are able to sense, process and analyze information and transfer it for further use. In addition, these distributed devices must harvest their energy from other means than batteries, as massive numbers of batteries mean massive end of life, waste disposal and recycling issues. The fabrication using low cost mass manufacturing processes allows wide application spectrum.

2. Experimental

The schematic structure of a flexible supercapacitor is shown in Fig. 1. In this work the total thickness of the capacitor with packaging was 0.6 - 0.8 mm and the length 50 – 80 mm. The width was normally 50 mm. The key technical requirements for current collectors are that they should have low resistance and the electrolyte should not corrode them. Together with current collectors the substrates form the package for the component. The package must prevent the evaporation of electrolyte and provide the required mechanical strength.

Paperboard Stora Enso Cupforma Classic Barr 20+190+42EB56 was used as one substrate material. When using paperboard substrates together with aluminium foil current collector, the foil was attached to the substrate using a spray coated adhesive layer. In addition, substrates of commercially available laminates consisting of aluminium and polyethylene terephthalate (PET) were tested. Ferric chloride was used to etch the current collector patterns, which are needed if the supercapacitor is made on a shared substrate with other components. Supercapacitors were also fabricated on substrates totally covered with aluminium to serve as discrete components. Fig. 2 shows two structures (A and B) on paperboard substrates and four components (C, D, E and F) made on PET based laminates. Two different Al/PET laminates were used. In the first one, supplied by Scandinavian Cable Service, the thicknesses of

aluminium and PET layers were 23 µm and 25 µm, respectively. A commercial grade substrate with 7 µm aluminium on 100 µm PET was purchased from CJI China Film and found to be preferable since the 7 µm aluminium layer can provide reasonably low resistance and the thicker PET provides better rigidity for the assembled component.

The graphite layer on the metal current collector (aluminium film or silver ink) has two functions: protection of the metal from corrosion in the case of aqueous electrolyte and reduction of contact resistance between metal and AC layer [31]. In all devices Acheson PF407C graphite ink was applied with doctor blade and cured at 95 ^{o}C for 1 hour. The AC ink contained 30.9 % AC powder, 1.7 % chitosan, 0.7 % acetic acid and 66.7 % water. Either Norit Super 30 or Kuraray YP-80F AC powder was used. The change was due to the cease in production of Norit Super 30 grade. The AC ink was applied on the graphite ink coated substrate using doctor blade coater and dried in ambient air in room temperature. In the experiments the geometrical AC layer area varied from 1 to 3.2 cm^2 and its thickness from 60 to 90 µm. An aqueous electrolyte (NaCl:H_2O with mass ratio 1:5) was used in all supercapacitors. Cellulose separators were used. The alternatives were NKK TF40 paper of 50 µm thickness and Dreamweaver Silver AR40.

The printed supercapacitor electrodes were assembled to components so that AC layers were face-to-face. A frame made of polyethylene (PE) was placed around the active layer and the separator to prevent short circuit between the two current collectors. For adhesion of the top and bottom electrodes, a hot melt foil Collano TEX-B 384 and Paramelt Aquaseal X2277 were used, as was the case with the AC, the changeover was necessary due to the end of availability of the first material.

The electrical properties of the supercapacitors such as capacitance, equivalent series resistance (ESR), and leakage current were determined using an industrial standard [32]. An Arbin SCTS instrument was used in the case of component types A, B, C and D and a Maccor 4300 with types E and F. The component was first charged and discharged with constant current up to 1.2 V three times, and then the voltage was kept for 30 minutes at 1.2 V and discharged with a constant current. The capacitance was defined during the constant current discharge step between 0.96 V and 0.48 V potential. The efficiency was defined as the ratio of the discharged and charged energy in the voltage range of 0 – 1.2 V or 0.2 – 1.2 V. The leakage current of the supercapacitors was determined with a float current experiment: the capacitor was charged to 1.2 V and the current recorded after holding that potential for 1 hour. For capacitor types E and F, self-discharge was also measured by charging the capacitors 1 h or 24 h with a constant voltage of 1.2 V, then disconnecting the capacitor from any outside circuits and manually checking the voltage level with a multimeter (input impedance 10 MΩ) for up to 26 days.

Table 1 shows the combination of substrates, current collectors, sealing and separator for each type of supercapacitor manufactured. The Dreamweaver separator replaced the NKK due to its higher mechanical strength when soaked with water. According to the manufacturer, NKK TF 40-50 is recommended mainly to be used with organic electrolytes. In component type F, the Al layer was on the outside of the supercapacitor, functioning only as barrier layer and not as current collector.

3. Results and discussion

The supercapacitors reported within this paper are listed in Table 2. The dimensions of the components varied slightly which must be taken into account for the comparison. The components can be divided to groups in various ways. One essential difference is the barrier type: in some components there is only PET together with graphite ink to prevent electrolyte evaporation or oxygen penetration from air to the

electrolyte. Some have aluminium layers in the substrate to enhance the tightness. Another important factor is the type of current collector.

Intuitively, the supercapacitors having either silver ink or aluminium foil to increase the current collector conductivity are expected to have lower ESR values. The disadvantage of this structure with an aqueous electrolyte is that the graphite ink layer between the metallic current collector and electrolyte must be dense enough to avoid corrosion. As a consequence of the electrolyte penetrating through the graphite ink layer after a few months we found visible signs of metal corrosion from a large number of the supercapacitors having this structure. The corrosion can be avoided by using graphite ink alone. The increase of ESR due to not using metallic materials can be partly tackled using the geometrical design described below.

3.1 Capacitance

The capacitance values of the supercapacitors are of the order of 0.05 – 0.6 F. Although two different AC inks were used (made of Norit or Kuraray AC powders) in the experiments, the variations are mainly due to changes in the geometrical area or thickness of the AC layer. The specific capacitance values measured for the cured Norit ink are 19-24 F/g and for cured Kuraray ink 26-29 F/g. These values apply for the total mass of the active electrode layers in the whole capacitor taking also the binder mass into account, i.e. for single electrode values these should be multiplied by a factor of four.

3.2 ESR

The equivalent series resistance (ESR) values for aluminium foil current collectors with aqueous electrolyte are of the same order as the ones obtained for silver ink current collectors, typically 0.4 – 1 Ω. Supercapacitors without the metallic current collector show considerably higher ESR. For a 25 µm thick layer of the graphite ink the square resistance is about 10 Ω as specified by the ink manufacturer for this particular production batch. To minimize ESR the geometry of supercapacitors with graphite

current collectors was modified. The current collectors were made wider and as short as possible. In this way ESR values of 10 – 15 Ω are obtained for current collector dimensions 30 mm x 30 mm and electrode dimensions 10 mm x 18 mm.

To further decrease the resistance without having the risk of metal corrosion, a new current collector layout was designed. A copper coated PET foil was used as substrate. Copper was etched from a 30 mm x 30 mm square. After the etching PF407C graphite ink was applied on the whole surface and on top of that in the middle of the underlying etched square a 14 mm x 14 mm AC electrode. After dispensing the electrolyte the component was sealed inside the etched square. The design ensures the electrolyte can´t get into contact with the copper layer while minimizing the distance of the copper from the active layer. This way an ESR of 5 Ω is reached.

NKK and Dreamweaver separators result to the same ESR values within general device to device fluctuations.

3.3 Efficiency

The energy efficiency of a supercapacitor correlates with ESR and leakage current. Typically, the higher the discharge and charge currents are, the more energy is lost due to ESR. When low current is used, relatively more energy may be lost due to the self-discharge of the supercapacitor. Fig. 3 shows the galvanostatic cycles that were used to define the energy efficiencies. The energy efficiencies in Table 2 were defined for all components with 10 mA charge and discharge current. Since the components of type E and F have higher ESR and are thus better suited for relatively low current applications, their efficiencies were defined also with 1 mA current.

3.4 Leakage current and self-discharge

Robust sealing of the capacitor device is essential not only to keep the electrolyte from escaping but also to prevent oxygen and other impurities from entering the device. Various methods for sealing the

Al/PET component were examined. Since PET requires quite high temperatures for heat sealing, it is necessary to use either a separate hot melt foil or to use an adhesive. With the hot melt foil a mechanically robust structure can be achieved.

Leakage current results in this case most likely from impurities which undergo Faradaic charge-transfer reactions at the electrodes. The impurities may be transition metal ions which are commonly found in carbon materials, or oxygen dissolved in the electrolyte and adsorbed on the surface on the activated carbon [1]. As the devices were assembled in ambient air, oxygen is likely to be present in the device. Other self-discharge mechanisms are electrolyte decomposition due to overcharge and direct Ohmic leakage due to imperfections in the construction of the supercapacitor [1].There is a clear correlation between the capacitance and leakage current as can be seen in Fig. 4. As the total surface area of the activated carbon in the device increases, the amount of adsorbed oxygen increases as well; on the other hand, the larger surface area increases the potential sites for faradaic leakage reactions to occur. The leakage current measured by the float current experiment (potential held constant) naturally shows some dependence also on the ESR, as a larger resistance reduces the measured current.

In the components belonging to groups A, C and E the leakage current values are typically 10 – 20 µA for most supercapacitors depending on the capacitance. The leakage current decreased by about 50 % after applying packaging with better barrier properties (components in groups B, D and F) leading to leakage currents in the range of 2 - 10 µA. The main difference is that in the new version the aluminium layer encapsulates the electrodes and electrolyte.

The self-discharge rate correlates with leakage current. In commercial supercapacitors the voltage decreases about 13-22 % during one month [2]. This corresponds to a voltage energy loss of about 25-39 %. Fig. 5 shows the self-discharge rate for supercapacitors of type E and F. The components were first

charged to 1.2 V and kept at that voltage for 1 hour. They were then disconnected from the voltage source and the open-circuit voltage was recorded after certain periods of time until the voltage had decreased to 0.9 V. After this test the same experiment was repeated except the constant voltage charging period was extended from 1 hour to 24 hours.

After improving the barrier properties of the package by using large area aluminium current collectors the self-discharge rate is significantly decreased. The improvement is believed to be due to decreased oxygen content in the electrolyte. [33]

The difference in self-discharge rate is substantial between capacitors charged for 1 h compared to 24 h. With the shorter charge, the activated carbon pore surfaces are not evenly covered with ions, with more ions at the pore openings than at the base [34,35]. When the charging step is finished, the ions migrate deeper into the pores; this charge redistribution causes the observed voltage of the capacitor to decline. With a longer charge of 24 h, the carbon pores become more evenly charged and the voltage declines more slowly. Such differences have been found previously between charging durations of 2 hours and 2 days [34]. Black and Andreas [35] have reported that hold steps of over 50 h are required to fully charge highly porous carbon electrodes.

The self-discharge mechanisms can be examined more closely through comparison to theoretical models predicting different rates for the process [36]. If the self-discharge occurs mainly through activation-controlled Faradaic reactions, V decreases linearly in $\log(t)$ or $\log(t+\tau)$. This is the case for both overcharge to a voltage where the electrolyte decomposes, and for reactions of impurities present in high concentrations or attached to the carbon surface [1,35]. When the leakage is through reactions of impurities present in sufficiently small concentrations, their diffusion to the electrodes becomes the limiting factor which determines the self-discharge rate. In this case, the voltage should fall linearly against the square root of time [36]. Another possible leakage source is a direct Ohmic leakage pathway

between the electrodes; this results in an exponential decay of the voltage over time, i.e. ln(V) falls linearly against t [36]. These three cases are examined in Fig. 6.

From the different type plots, it can clearly be seen that in supercapacitor F1 the voltage decline is linear in log($t+\tau$), suggesting that the leakage is through Faradaic reactions. This is expected, as the supercapacitors were assembled in ambient air, resulting in high impurity content in the device. Supercapacitor type E is not as clearly one type of discharge, the voltage fall not being strictly linear in any of the cases. It is close to linear in Fig. 6b, but the leakage is unlikely to really be diffusion-limited because in type F it was not either. The voltage fall is rapid compared to type F, where there is an Al barrier layer. As the measurement time period is over a month, it is likely that more impurities, probably oxygen, are entering the supercapacitor. The Ohmic leakage case, Fig. 6c, appears close to linear after the first few days, but it is unlikely to be the mechanism here, because samples E1 and E2 displayed similar behaviour; if short circuits between the electrodes had arisen due to assembly imperfections, this would be unlikely to induce similar resistance in both samples.

The leakage is thus most likely due to Faradaic reactions of impurities in the supercapacitors. The leakage may be reduced by e.g. vacuum treating the electrodes prior to assembly to reduce the amount of adsorbed oxygen, or bubbling the electrolyte with inert gas to remove dissolved oxygen. The purity of the activated carbon material is one critical aspect as well, due to both surface functional groups and transition metal trace impurities which can be quite common in many carbons [1].

3.5 Lifetime

The evaporation rate of electrolyte was estimated by weighing the supercapacitors after the assembly during a few weeks. The amount of electrolyte in the components was approximately 200 mg. Since the water gets evaporated through the package, the salt concentration increases in the electrolyte resulting in saturation and salt crystallization. This prevents the formation of the electric double layer on the

electrode surface which decreases the capacitance of the component. The ionic conductivity is also reduced due to salt crystallization. Another consequence of the evaporation of water is that parts of the carbon surface may not be in contact with the electrolyte, making them inoperative and thus decreasing the capacitance.

The weight loss in the case of graphite ink coated Cupforma Barr is about 5 mg/week which restricts the component lifetime to a few months. The evaporation rate through graphite ink coated 100 µm thick PET foil is of about the same order. By using the Al/PET laminates the evaporation rate can be drastically reduced. For the components with large aluminium layer covering the whole electrolyte area we have measured evaporation rates of 0.01-0.3 mg/week. The variation may be due to the fact that some evaporation takes place through the sealing material. If the electrolyte loss was the life-time limiting factor, with the aluminium barrier packaging the life-time would be several years.

A cycle life test with 20 mA current between 0.2 and 1.2V was performed for sample D4. Its initial capacitance was 0.450 F. The percent change of capacitance and energy efficiency as a function of cycle count is shown in Fig. 7. As can be seen, the capacitance value decreases to about 91 % of the original value during 40000 cycles. Simultaneously the efficiency decreases from 96 % to 90 %, with leakage current gradually decreasing. The decrease in leakage current with cycle number can be explained by increase in penetration of ions to pores in the electrode with successive charging cycles, which is the same effect as discussed above with regard to dependence of self-discharge rate on charging time.

3.6. Application potential

All of the structures presented are feasible for practical applications, and the choice of architecture depends on the requirements for the stored energy content and output power. As an example, in a case where 100 mV voltage loss would be acceptable and the geometrical electrode area is 2 cm^2, supercapacitors of types A, B, C and D with their ESR of about 1 Ω would allow about 100 mA output

current correspoinding 100 mW with 1 V potential. With similar constraints the supercapacitors of type E can be used to provide about 20 mW and type F about 10 mW power. Beside power requirements, the choice of supercapacitor type can be made according to materials used in other parts of the system. E.g. in packages made of paperboard the types A and B may result to cost savings. To avoid the metal corrosion risk caused by electrolyte going through the graphite ink, types E and F can be recommended. Further, to avoid the shortening of lifetime caused by electrolyte evaporation or to minimize leakage current due to oxygen penetration through the package to electrolyte, the structure alternatives with barrier layer (B, D and F) are recommended. If long life-time and high power are needed in the same supercapacitor, more work is still needed to find a means to provide adequate corrosion protection for metal current collectors. For lower power applications where slightly higher ESR is acceptable corrosion-resistant architectures as reported in this paper are suitable. Examples of suitable applications for our supercapacitors include autonomous energy systems together with e.g. piezoelectric or RF harvester [16, 17].

4. Conclusions

Performance of flexible supercapacitors with different architectures and material selections were thoroughly studied in this work. Devices were prepared using paperboard or PET substrate materials, activated carbon active layers, current collectors from graphite ink and metal (aluminum or copper) films, and aqueous NaCl electrolyte. The device capacitance varied from 85 mF to 580 mF. In particular it was found that ESR, which varied from 1 Ω to 14 Ω, mainly depends on the current collector structure and materials. Furthermore, the device encapsulation had significant effect on the leakage currents, which varied from 2 µA to 20 µA. This effect was most dramatic in devices with an aluminium barrier layer that exhibited leakage currents about 50 % smaller than the other devices. The self-discharge rate of the supercapacitors correlates with the leakage current, which is mostly due to Faradaic reactions of

impurities in the electrode layers when an aluminium barrier layer is used. In general, the leakage current also decreased during the charge/discharge cycling tests. In these cycle life tests, the device capacitance showed less than 10 % decrease in the capacitance after 40 000 charge-discharge cycles.

Acknowledgements

Financing from Tekes – the Finnish Funding Agency for Innovation including decisions 40146/14, 40337/14, 40044/12, and 40109/10 is greatly acknowledged.

References

1. B. E. Conway, *Electrochemical Supercapacitors: Scientific Fundamentals and Technological Applications*, Springer US, Boston, MA (1999).

2. M. Lu, F. Béguin, and E. Frąckowiak, *Supercapacitors: Materials, Systems, and Applications*, Wiley-VCH Verlag GmbH & Co. KGaA, Weinheim, Germany (2013).

3. R. Moscatiello, *SGIA J. (1st Quarter)* 25 (2005).

4. B. Dyatkin, V. Presser, M. Heon, M. R. Lukatskaya, M. Beidaghi, and Y. Gogotsi, *ChemSusChem* **6**, 2269 (2013).

5. J. Keskinen, E. Sivonen, S. Jussila, M. Bergelin, M. Johansson, A. Vaari, and M. Smolander, *Electrochim. Acta* **85**, 302 (2012).

6. S. Lehtimäki, S. Tuukkanen, J. Pörhönen, P. Moilanen, J. Virtanen, M. Honkanen, and D. Lupo, *Appl. Phys. A* **117**, 1329 (2014).

7. K. Torvinen, S. Lehtimäki, J. T. Keränen, J. Sievänen, J. Vartiainen, E. Hellén, D. Lupo, and S. Tuukkanen, *Electron. Mater. Lett.* **11**, 1040 (2015).

8. J. Keskinen, E. Sivonen, M. Bergelin, J. E. Eriksson, P. Sjöberg-Eerola, M. Valkiainen, M. Smolander, A. Vaari, J. Uotila, H. Boer, and S. Tuurala, *Adv. Sci. Technol.* **72**, 331 (2010).

9. B. C. Kim, J.-Y. Hong, G. G. Wallace, and H. S. Park, *Adv. Energy Mater.* **5**, n/a (2015).

10. A. El Hajj, T. M. Kraft, B. Lucas, M. Schirr-Bonnans, B. Ratier, and P. Torchio, *J. Appl. Phys.* **115**, 033103 (2014).

11. Y. H. Lee, J. S. Kim, J. Noh, I. Lee, H. J. Kim, S. Choi, J. Seo, S. Jeon, T. S. Kim, J. Y. Lee, and J. W. Choi, *Nano Lett.* **13**, 5753 (2013).

12. Z. Cui, F. R. Poblete, G. Cheng, S. Yao, X. Jiang, and Y. Zhu, *J. Mater. Res.* **30**, 79 (2015).

13. J. Bae, M. K. Song, Y. J. Park, J. M. Kim, M. Liu, and Z. L. Wang, *Angew. Chemie - Int. Ed.* **50**, 1683 (2011).

14. Z. Yang, J. Deng, X. Chen, J. Ren, and H. Peng, *Angew. Chemie - Int. Ed.* **52**, 13453 (2013).

15. T. Kim, H. Song, J. Ha, S. Kim, D. Kim, S. Chung, J. Lee, and Y. Hong, *Appl. Phys. Lett.* **104**, 113103 (2014).

16. J. Pörhönen, S. Rajala, S. Lehtimäki, and S. Tuukkanen, *IEEE Trans. Electron Devices* **61**, 3303 (2014).

17. S. Lehtimäki, M. Li, J. Salomaa, J. Pörhönen, A. Kalanti, S. Tuukkanen, P. Heljo, K. Halonen, and D. Lupo, *Int. J. Electr. Power Energy Syst.* **58**, 42 (2014).

18. F. Pettersson, J. Keskinen, T. Remonen, L. von Hertzen, E. Jansson, K. Tappura, Y. Zhang, C.-E. Wilén, and R. Österbacka, *J. Power Sources* **271**, 298 (2014).

19. D. Wei, S. J. Wakeham, T. Wing, M. J. Thwaites, H. Brown, P. Beecher, T. W. Ng, M. J. Thwaites, H.

Brown, and P. Beecher, *Electrochem. Commun.* **11**, 2285 (2009).

20. M. Kaempgen, C. K. Chan, J. Ma, Y. Cui, and G. Gruner, *Nano Lett.* **9**, 1872 (2009).

21. K. Jost, C. R. Perez, J. K. McDonough, V. Presser, M. Heon, G. Dion, and Y. Gogotsi, *Energy Environ. Sci.* **4**, 5060 (2011).

22. L. Hu, H. Wu, and Y. Cui, *Appl. Phys. Lett.* **96**, 183502 (2010).

23. L. T. Le, M. H. Ervin, H. Qiu, B. E. Fuchs, and W. Y. Lee, *Electrochem. Commun.* **13**, 355 (2011).

24. P. Kossyrev, *J. Power Sources* **201**, 347 (2012).

25. S. Lawes, A. Riese, Q. Sun, N. Cheng, and X. Sun, *Carbon N. Y.* **92**, 150 (2015).

26. O. S. Nissen, H. C. Beck, and M. Schou, Patent No. 6,341,057. (2002).

27. J. Lang, US Patent 6937460 B2 (2005).

28. C. Z. Meng, C. H. Liu, L. Z. Chen, C. H. Hu, and S. S. Fan, *Nano Lett.* **10**, 4025 (2010).

29. J. Keskinen, S. Tuurala, M. Sjödin, K. Kiri, L. Nyholm, T. Flyktman, M. Strømme, and M. Smolander, *Synth. Met.* **203**, 192 (2015).

30. V. L. Pushparaj, M. M. Shaijumon, A. Kumar, S. Murugesan, L. Ci, R. Vajtai, R. J. Linhardt, O. Nalamasu, and P. M. Ajayan, *Proc. Natl. Acad. Sci. U. S. A.* **104**, 13574 (2007).

31. C. Portet, P. L. Taberna, P. Simon, and C. Laberty-Robert, *Electrochim. Acta* **49**, 905 (2004).

32. *International Standard: Fixed Electric Double Layer Capacitors for Use in Electronic Equipment, IEC 62391-2-1*, (2006).

33. M. Hahn, P. Furrer, B. Schnyder, M. Baertsch, R. Koetz, O. Haas, C. Ohler, and M. W. Carlen, in

Proc. 10th Int. Semin. Double Layer Capacit. Similar Energy Storage Devices Deerfield Beach, Florida, USA (2000), pp. 1–12.

34. M. Kaus, J. Kowal, and D. U. Sauer, *Electrochim. Acta* **55**, 7516 (2010).

35. J. Black, and H. Andreas, *Electrochim. Acta* **54**, 3568 (2009).

36. B. E. Conway, W. G. Pell, and T.-C. Liu, *J. Power Sources* **65**, 53 (1997).

Table 1. Supercapacitor types.

Type	**Substrate**	**Current collector**	**Activated carbon**	**Sealing**	**Separator**	**Al barrier**
A	Paperboard	Ag-ink + graphite ink	Norit	Collano	NKK	No
B	Paperboard	Al-foil + graphite ink	Norit	Collano	NKK	Yes
C	Al23/PET25	Al from substrate+graphite ink	Norit	Collano	NKK	No
D	Al7/PET100	Al from substrate+graphite ink	Norit	Collano	NKK	Yes
E	Cu/PET125	100 nm evaporated Cu + graphite ink	Kuraray	Paramelt	Dreamweaver	No
F	PET50/Al9, electrode on PET side	Graphite ink	Kuraray	Paramelt	Dreamweaver	Yes

Table 2. List of prepared supercapacitor samples with their properties and performance.

Code/ Sample	Area (cm^2)	Current (mA)	Capacitance (F)	Capacitance/ area (F/cm^2)	Energy efficiency (%)	Leakage current (µA)	ESR ()Ω
A1	2	10	0.32	0.16	94	12	1.0
A2	2	10	0.28	0.14	96	10	0.9
A3	2	10	0.32	0.16	95	12	1.0
A4	2	10	0.20	0.1	95	12	1.0
A5	2	10	0.14	0.07	96	15	0.7
A6	2	10	0.33	0.17	96	10	0.8
B1	1	10	0.085	0.085	90	2.3	3.0
B2	1	10	0.1	0.1	90	1.3	3.5
B3	1	10	0.32	0.32	91	3.5	1.5
B4	1	10	0.27	0.27	89	5.5	1.5
B5	1	10	0.26	0.26	88	3.9	1.7
C1	2	10	0.51	0.256	93	20	0.9
C2	2	10	0.58	0.29	92	15	0.8
C3	2	10	0.45	0.23	92	14	1.1
D1	1	10	0.048	0.048	91	2.5	3.0
D2	2	10	0.39	0.20	94	6.3	1.3
D3	2	10	0.36	0.18	92	8.5	2.0
D4	3.2	10	0.45	0.14	96	8	0.8
E1	2	1	0.48	0.24	93	14	5.3
		10	0.45	0.23	77		

E2	2	1	0.50	0.25	92	16.5	5.4
		10	0.47	0.24	75		
F1	1.8	1	0.30	0.17	86	7	14
		10	0.24	0.13	59		
F2	1.8	1	0.28	0.16	84	6.5	12
		10	0.21	0.12	54		
F3	1.8	1	0.34	0.19	93	9.5	10
		10	0.28	0.16	63		
F4	1.8	1	0.34	0.19	93	9	10
		10	0.32	0.18	69		

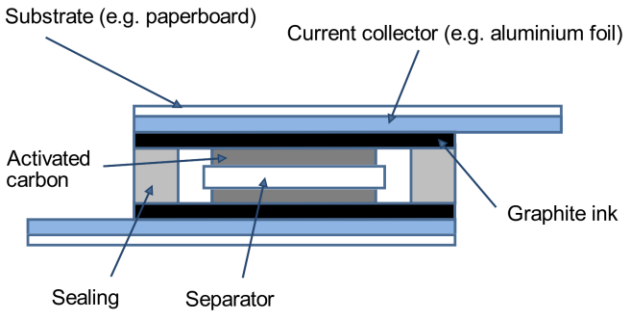

Fig. 1. Schematic side-view of a printed supercapacitor. The horizontal and vertical dimensions are not in the scale.

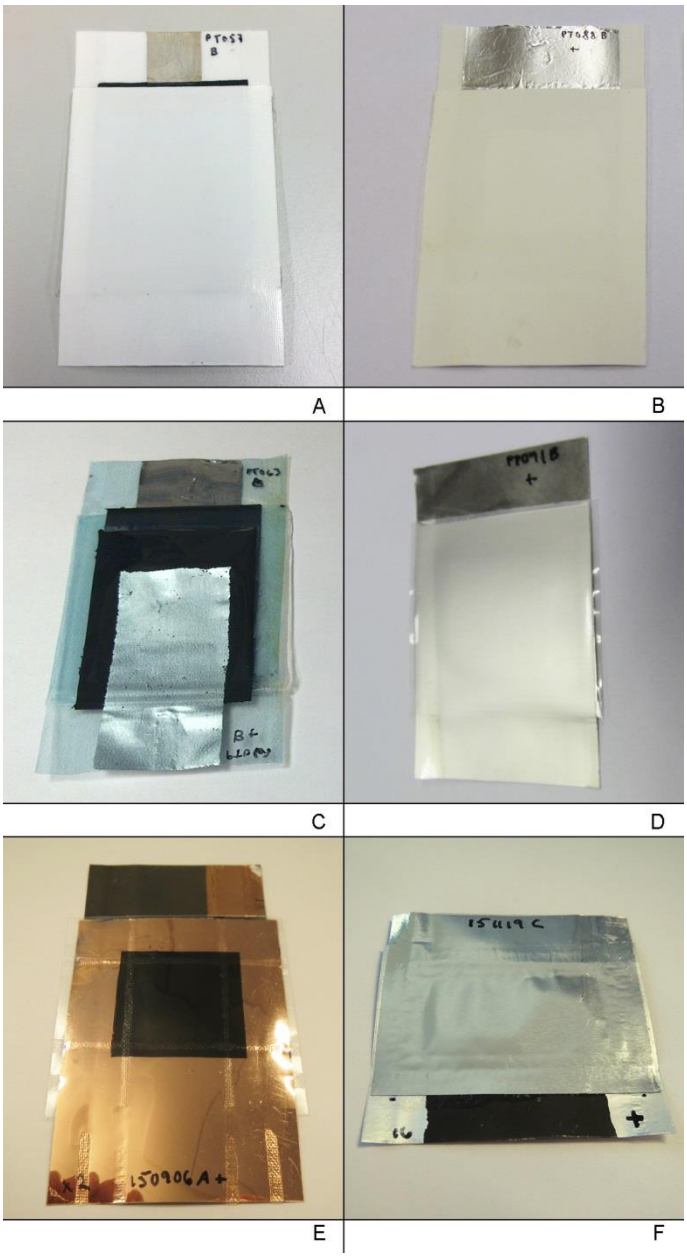

Fig. 2. Photographs of supercapacitors. The letters A-F refer to the codes in Table 1. The width of all components is 50 mm.

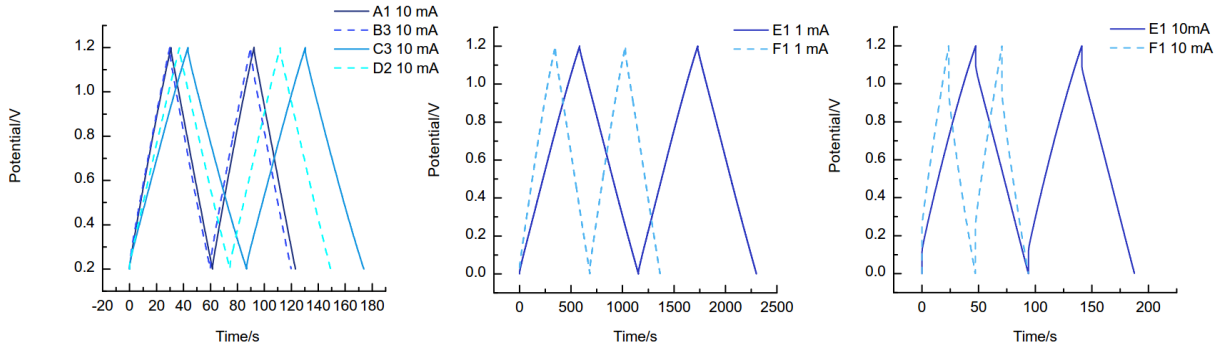

Fig. 3. Charge-discharge cycles measured with constant 10 mA and 1 mA current.

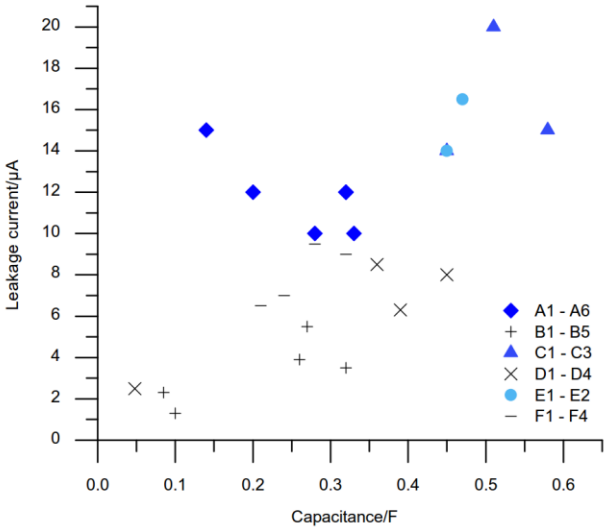

Fig. 4. Leakage current of supercapacitors as a function of capacitance.

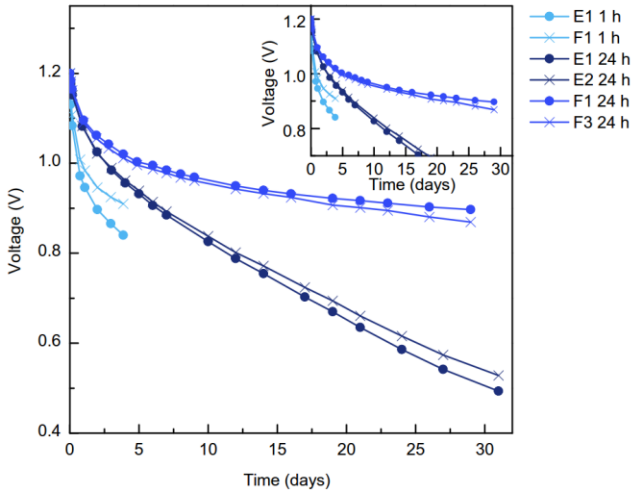

Fig. 5. Self-discharge rate of supercapacitors of type E and F. Type E substrate is 125 µm thick PET with additional copper current collectors outside the sealed area, type F 50 µm thick PET with aluminium barrier layer on the outside.

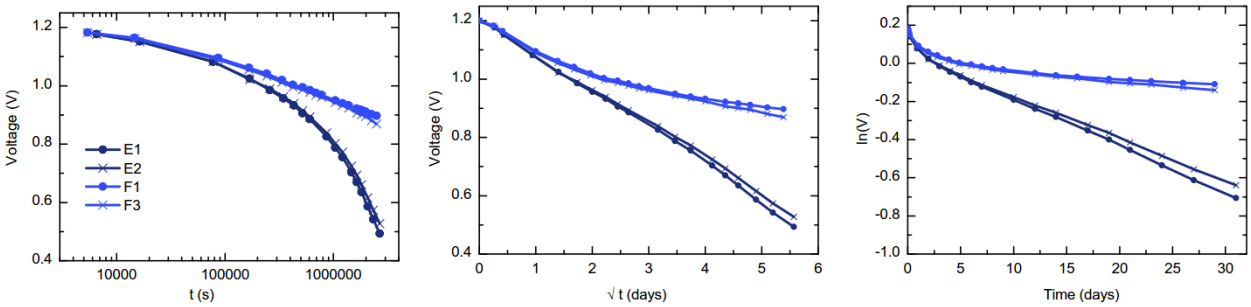

Fig. 6. Self-discharge of supercapacitors type E and F plotted with (a) V vs. log(t), (b) V vs. √t, (c) ln(V) vs.t, relating to leakage through Faradaic, diffusion-limited and Ohmic mechanisms, respectively. The dark lines are measurements with 1 h charge time and the light lines with 24 h charge time.

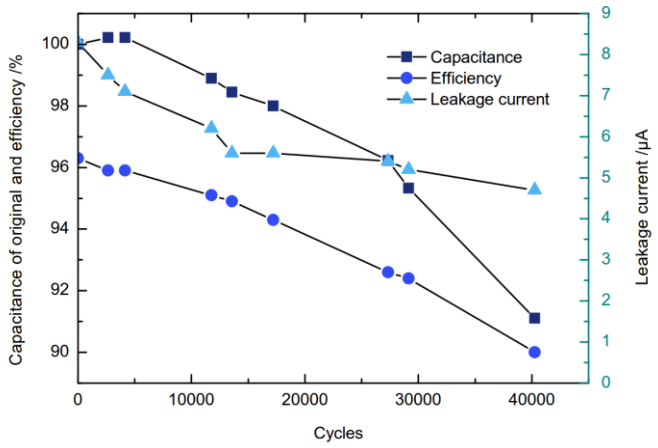

Fig. 7. Capacitance, efficiency and leakage current as a function of the number of charge-discharge cycles for supercapacitor D4.

TOC Figure

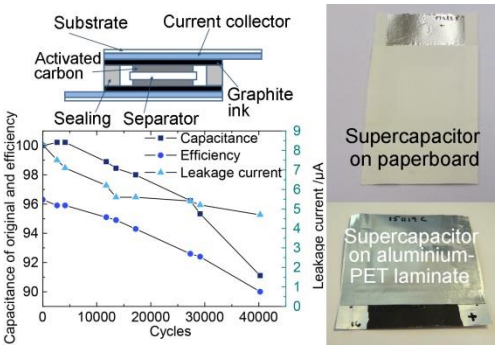
Substrate
Current collector
Activated carbon
Graphite ink
Sealing
Separator
Capacitance
Efficiency
Leakage current
Capacitance of original and efficiency
Leakage current /μA
Cycles
0
10000
20000
30000
40000
90
92
94
96
98
100
0
1
2
3
4
5
6
7
8
9
Supercapacitor on paperboard
Supercapacitor on aluminium-PET laminate